A direct comparison of vibrational deactivation of hexafluorobenzene excited by infrared multiple photon absorption and internal conversion

Jason R. Gascooke
Department of Chemistry, Flinders University, G.P.O Box 2100, Adelaide SA 5001, Australia

Zeyad T. Alwahabi and Keith D. King[a)]
Department of Chemical Engineering, University of Adelaide, SA 5005 Australia

Warren D. Lawrance
Department of Chemistry, Flinders University, G.P.O. Box 2100, Adelaide SA 5001, Australia

(Received 7 April 1998; accepted 5 June 1998)

We report the first direct comparison between energy transfer parameters measured using infrared multiphoton absorption (IRMPA) versus ultraviolet (UV) excitation followed by rapid internal conversion (IC). Highly excited hexafluorobenzene (HFB) molecules in the electronic ground state were prepared by (i) IRMPA by CO_2 laser pumping to an average initial energy of 14 500–17 500 cm^{-1} and (ii) UV excitation to ~40 300 cm^{-1} followed by IC. The vibrational deactivation of the highly excited HFB by the monatomic collider gas argon was monitored by time-resolved infrared fluorescence. The results for the two methods are identical within experimental error, demonstrating the viability of IRMPA as a method of state preparation for vibrational deactivation experiments involving large molecules. © *1998 American Institute of Physics.* [S0021-9606(98)01934-5]

I. INTRODUCTION

Direct measurements of collisional energy transfer from highly excited gas phase molecules usually rely on ultraviolet (UV) pumping of a molecule to an excited electronic state, followed by non-radiative intramolecular transfer to high-lying vibrational levels in the ground electronic state as the means of state preparation.[1] Producing an ensemble of excited molecules through rapid internal conversion (IC) has the advantage that the initial energy distribution is extremely narrow and defined, centered about the excitation wavelength of the light source used. This technique, however, is limited to molecules possessing an electronic transition which will undergo rapid internal conversion at wavelengths accessible by conventional lasers. Consequently the range of initial internal energies that can be studied is severely restricted by the energy of the electronic transitions.

Infrared multiphoton absorption (IRMPA), generally using a high power CO_2 laser, provides an alternative method for initial preparation of large populations of highly excited molecules in the ground electronic state with various initial internal energies.[2–9] In contrast with studies utilizing UV pumping followed by IC, IRMPA remains a poor cousin. This arises because there is uncertainty in the initial energy distribution associated with the IRMPA process.[3–6] Nevertheless, it has been shown theoretically that under appropriate conditions the results extracted from the data depend solely on the *average* excitation energy, i.e., they are independent of the initial distribution.[10,11] The average internal energy the excited molecule initially reaches after IRMPA is controlled by varying the fluence of the excitation laser.

IRMPA is potentially a very useful technique for studying different types of molecular systems from those studied using IC as the state preparation technique. IC following visible/UV excitation has generally been used with cyclic ring systems, usually aromatics, because these molecules possess the required photophysical properties. In contrast, molecules studied using IRMPA are halogenated hydrocarbons, for example 1,1,2-trifluoroethane,[6] *cis*-ClFC=CFCl (Ref. 9) and $CDCl_3$.[12] It is clear that the types of molecules for which direct energy transfer data are available need to encompass a broader range of systems, and this is not possible using the IC technique for state preparation. IRMPA offers a versatile alternative.

In order to remove the stigma associated with using IRMPA for excitation so that it can reach its full potential, it is necessary to demonstrate that the drawbacks identified above are no impediment to obtaining high quality data. For this reason we have undertaken a study of energy transfer in hexafluorobenzene (HFB), for which it is possible to use both IRMPA and IC as methods of excitation. Argon was used as the collision partner. By comparing the results of these studies we aim to demonstrate the reliability of results obtained with IRMPA. Our experimental results are compared with previous experimental work[13] and with recent quasiclassical trajectory calculations on the deactivation of highly excited HFB by some mono and polyatomic collision partners.[14,15]

II. EXPERIMENT

HFB has two very strong infrared (IR) absorption bands centered around 1007 and 1530 cm^{-1}, the former being coincident with CO_2 laser output. We use time-resolved infra-

a)Electronic mail: kking@chemeng.adelaide.edu.au

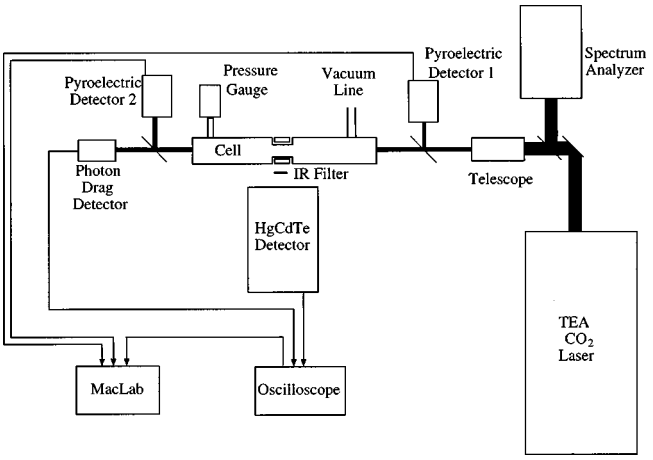

FIG. 1. Schematic diagram of the experimental system.

red fluorescence (IRF) near 1500 cm^{-1} to monitor energy loss from highly vibrationally excited HFB prepared by IRMPA with CO_2 laser pumping using the $P(38)$ line at 1029.43 cm^{-1}. The IC-IRF experiments utilized 248 nm ($\sim$40 300 cm^{-1}) excitation. Due to it providing superior signals, the band near the 1000 cm^{-1} band was monitored in these UV excitation experiments.

The experimental system for the excitation of HFB via IRMPA coupled with time-resolved IRF monitoring is a more elaborate version of the experimental design used for recent studies of the collisional deactivation of vibrationally excited CO_2 and N_2O.[16–18] A schematic diagram of the experimental arrangement is shown in Fig. 1. Infrared laser radiation from a tunable CO_2 laser (Lumonics TEA 103-2) is directed through a Galilean telescope and then into a cylindrical fluorescence cell constructed from stainless steel and fitted with NaCl end windows. A mercury-free gas handling line can evacuate the cell to $\sim 10^{-4}$ Torr. The pressure in the cell was monitored with a 0–1 Torr capacitance manometer (MKS Baratron). The IRF from the excited HFB molecules was observed perpendicular to the laser beam axis through a MgF_2 side window and a bandpass interference filter centered at 1486 cm^{-1} with a band width of 167 cm^{-1}. The IRF is detected with a liquid nitrogen cooled HgCdTe detector (Infrared Associates) equipped with a matched preamplifier (combined rise time $\sim$400 ns). The detector/preamplifier output was captured by a digital storage oscilloscope (LeCroy 9310) and transferred to a laboratory computer for analysis. The detector/preamplifier was shielded by a copper cage to prevent electrical interference from the firing of the laser.

A photon drag detector (Rofin 7415) was used to monitor the CO_2 laser pulse temporal profile and to trigger the oscilloscope. The oscilloscope was used to average decay curves for $\sim$200 pulses at a laser pulse repetition frequency of $\sim$1 Hz, in order to achieve adequate signal-to-noise ratios.

Extreme care was taken in the measurements of the average number of IR photons absorbed per HFB molecule. The conventional method involves averaging the energy of the CO_2 laser before and after the sample.[19] In our experiments, the energy of each pulse before and after the cell was recorded simultaneously using two pyroelectric joulemeters (Molectron J25). The signal from these joulemeters was captured using a data acquisition system (MacLab/4) allowing every shot to be recorded. This allows the energy absorbed, and hence the average number of photons absorbed per molecule, to be determined for every pulse. This is then repeated over a number of pulses to obtain the average number of photons absorbed per molecule and also an indication of the spread in initial excitation energies. Furthermore, the CO_2 laser was optimized for pulse-to-pulse stability and the triggering system of the IR detection system was set up so that it accepted signal only when the laser fluence was above a preset threshold. This results in optimum pulse to pulse stability and narrow distribution of the energy input. The laser beam was checked regularly for uniformity to ensure no hot spots were present. Consequently the initial excitation energy does not vary significantly from shot to shot.

In the experiments using UV excitation coupled with time-resolved IRF monitoring, the HFB was irradiated by an excimer laser (Questek Model 2220) at $\lambda = 248$ nm (KrF) operating at 10 Hz. The cell was fitted with quartz end windows to allow the transmission of the UV laser. The excimer pulses had an average fluence of $\sim$4 mJ cm^{-2} and a full width half maximum (FWHM) of 10 ns. Low laser power was necessary to prevent the deposition of polymer products on the cell windows which contributed to large amounts of scattered light. IRF from HFB near 1000 cm^{-1} was monitored through a NaCl window and appropriate bandpass interference filter with the HgCdTe detector coupled to a digital storage oscilloscope (Hewlett–Packard 54510A). Approximately 1000 laser shots were averaged for each run to obtain adequate signal-to-noise.

Ar (BOC 99.997%) was used directly as supplied. C_6F_6 (Aldrich, 99%) was degassed using several freeze–pump–thaw cycles prior to use.

III. DATA ANALYSIS

A. Variation of internal energy with time

The experiments measure infrared intensity as a function of time. From these data one wishes to extract the variation of the internal energy with time. The usual methods for doing this have been described by Barker.[20,21] They involve extrapolating the experimental intensity versus time traces to time zero where the initial energy is known. The changes in IR fluorescence intensity with time can then be associated with changes in internal energy with time using calculated calibration curves (see below). The accuracy of this method relies on the accuracy of the back-extrapolation, and ignores problems such as the finite detector response.

Our experience with the back extrapolation approach has been that it can lead to larger uncertainties than the data warrant. For this reason we have chosen a different approach that overcomes the limitations of back-extrapolation and allows effects such as the finite detector response to be incorporated in the analysis. The method involves fitting the internal energy versus time behavior directly to the data.

The internal energy is assumed to follow the general functional form:

$$E(t)=E_0\ \exp[-k_{t_1}(t-t_0)-k_{t_2}(t-t_0)^2], \tag{1}$$

where E_0 is the initial excitation energy and k_{t_1}, k_{t_2}, and t_0 are variable parameters in the fitting procedure. (It should be noted that this functional form is only a mathematical representation of the energy decay profile used for fitting purposes and there is no physical meaning associated with the parameters k_{t_1} and k_{t_2}). This functional form was chosen since an exponential is the most widely used form for modeling energy decay and, through the presence of a second t^2 term, the expression additionally allows for the roll-off in the average energy transferred per collision as reported by previous workers.[13,20,21] The procedure involves the following five steps:

(1) An initial set of k_{t_1}, k_{t_2}, and k_0 parameters is used to generate an $E(t)$ function, as per Eq. (1).

(2) This $E(t)$ function is converted to an infrared fluorescence intensity versus time function, IRF(t), using the relationship between relative IRF intensity of the nth mode, $I_n(E)$, and internal energy, first derived by Durana and McDonald:[22]

$$I_n(E)=\sum_{v=1}^{v_{\max}} v\ \frac{\rho_{s-1}(E-vh\nu_n)}{\rho_s(E)}, \tag{2}$$

and

$$\mathrm{IRF}(t)=A_{\mathrm{IRF}}I_n[E(t)]. \tag{3}$$

Here $h\nu_n$ is the energy of the nth mode, $\rho_s(E)$ is the vibrational density of states at energy E, $\rho_{s-1}(E)$ is the vibrational density of states calculated by excluding the mode that is being monitored and A_{IRF} is a fitted scaling factor. The applicability of the above relationship has been extensively tested and no occurrences have been found where the relationship has failed to hold.[23] The density of states were calculated using an exact counting algorithm[24] and the vibrational frequencies listed by Steele *et al.*[25,26]

(3) An infrared emission versus time curve is generated from the IR fluorescence intensity versus time function calculated at step (2), IRF(t), and a function used to describe blackbody radiation. This is necessary as in general the infrared emission signal contains components from both IRF and blackbody radiation (present due to the generation of heat during the collisional relaxation process). Thus the experimental decays consist of a superposition of an IRF decay curve and a blackbody radiation rise. The blackbody radiation, BBR(t), was represented by an expression which is derived from the standard BBR formulae:[27]

$$\mathrm{BBR}(t)=A_{\mathrm{BBR}}\ \exp\left(-\frac{h\nu}{kT(t)}\right), \tag{4}$$

and

$$T(t)=T_0+\Delta T\left(1-\frac{E(t)}{E_0}\right), \tag{5}$$

where A_{BBR} is an intensity constant, T_0 is the initial temperature, ΔT is the temperature rise after relaxation, and E_0 is the initial vibrational energy. The short timescales used throughout these experiments precluded the need to consider the slow decay of heat to the cell walls. The infrared emission intensity is thus:

$$\mathrm{IR}(t)=\mathrm{IRF}(t)+\mathrm{BBR}(t). \tag{6}$$

In principle, A_{BBR} and ΔT are both adjustable parameters introduced by the addition of blackbody radiation. However, in practice A_{BBR} is the only adjustable parameter required as the calculations were found to be insensitive to ΔT over a wide range of values (e.g., ~20–200 K rise in our results).

(4) The calculated infrared emission signal, IR(t), is convoluted with the detector response function, SRF(t), determined experimentally:

$$I(t)=\mathrm{SRF}(t)*\mathrm{IR}(t). \tag{7}$$

$I(t)$ is thus a calculated function that can be compared directly with the observed IR emission traces.

(5) $I(t)$ is compared with the experimental trace, the parameters k_{t_1}, k_{t_2}, t_0, A_{BBR}, and A_{IRF} are adjusted, and the process repeated until the calculated and experimental traces converge. In practice the entire process is automated. We used the Levenberg–Marquardt method of nonlinear least-squares fitting to match an $E(t)$ function to an observed IR emission trace.[28,29]

TABLE I. Lennard-Jones parameters used in this study.

Collider	σ (Å)	ϵ/k_b (K)	$10^{10}k^{\mathrm{LJ}}$ ($\mathrm{cm^3\ s^{-1}}$)
Ar	3.47	113.5	4.151
HFB	6.19	323	5.208

B. Extraction of energy transferred per collision as a function of internal energy

The decay curves are measured at a range of HFB dilutions in the collider gas. For each curve, i.e., each dilution, values of k_{t_1} and k_{t_2} are determined as discussed in Sec. III A, giving an $E(t)$ function. This expression for $E(t)$ is converted to $E(z)$, where z is the collision number determined using Lennard-Jones collision frequencies.[14] Lennard-Jones parameters used in our work, shown in Table I, are the same as those used in previous HFB energy transfer studies.[13,14] The values for k^{LJ} were calculated using the empirical formulae given by Neufeld *et al.*[30] for the collision integral. The form of $E(z)$ thus obtained is analytic [since $E(t)$ is analytic from Eq. (1)], and an expression is readily derived for $dE(z)/dz$, the average energy transferred per collision, $\langle\langle\Delta E\rangle\rangle$. Using Eq. (1), the functional form for the average energy transferred per collision is given by:

$$\langle\langle\Delta E\rangle\rangle=-\langle\langle E\rangle\rangle[k_{z_1}^2-4k_{z_2}\ \ln(\langle\langle E\rangle\rangle/E_0)]^{1/2}, \tag{8}$$

where k_{z_1} and k_{z_2} are related to k_{t_1} and k_{t_2} via the transformation from time to collision number. These $\langle\langle\Delta E\rangle\rangle$ functions refer to particular mixtures of HFB and collision partner and thus include both HFB-HFB collisions and HFB-collision partner collisions. To extract the HFB-collision partner value alone, these $\langle\langle\Delta E\rangle\rangle$ functions must be extrapo-

lated to the case of infinite dilution of HFB in the collision partner. This is achieved by plotting $\langle\langle \Delta E \rangle\rangle$ as a function of the collision fraction, F_c, for a series of energy values (typically every 250 cm^{-1}). The collision fraction is given by

$$F_c = \frac{k_c^{LJ} N_c}{k_c^{LJ} N_c + k_p^{LJ} N_p}, \tag{9}$$

where k_c^{LJ} and k_p^{LJ} are the Lennard-Jones collision frequencies of the HFB–Ar and HFB–HFB, pair respectively, and N_c and N_p are the number of collider and parent molecules, respectively. By extrapolating each $\langle\langle \Delta E \rangle\rangle$ vs F_c plot to $F_c = 1$, a $\langle\langle \Delta E \rangle\rangle$ value corresponding solely to HFB-collision partner energy transfer is obtained at each energy, $\langle\langle E \rangle\rangle$. These points obtained using this method were fitted using the following functional form to obtain the final $\langle\langle \Delta E \rangle\rangle$ vs $\langle\langle E \rangle\rangle$ curve:

$$\langle\langle \Delta E \rangle\rangle = -\langle\langle E \rangle\rangle [k_1^2 - 4k_2 \ln(\langle\langle E \rangle\rangle / E_0)]^{1/2}. \tag{10}$$

IV. RESULTS

A. IRMPA–IRF experiments

While IRMPA is an extremely useful method for preparing an initial ensemble of highly excited molecules at variable initial internal energies, it leads to a range of initial energies since molecules within the sample can absorb an integer number of photons, ranging from zero up. Various workers have either calculated this distribution[3–6] or it has been inferred using experimental techniques such as Raman spectroscopy.[31,32] Problems arise as the distribution can be bimodal, resulting from a near thermal population of those molecules that did not absorb, and a higher energy distribution of molecules that absorbed many photons.[19] The average number of photons absorbed per molecule, $\overline{n}$, is determined from the total energy absorbed by the molecules, and the number of absorbing molecules. In the case of the bimodal distribution just discussed, a calculation of $\overline{n}$, and hence the average initial vibrational energy, requires a knowledge of the fraction of molecules that underwent the IRMPA process.

In general the fraction of molecules excited increases with increasing laser fluence.[19] To produce significant levels of internal excitation, high fluences are required so that many photons are absorbed. Thus energy transfer experiments typically operate under conditions in which the molecules remaining in the unexcited thermal fraction constitute a small component. Indeed, for large molecules where the quasicontinuum is reached easily, the fraction of molecules left in the thermal component can be negligible.

In the case of HFB there are two previous experimental measurements suggesting that essentially all of the molecules are excited by the CO_2 laser.[33,34] The evidence consists of UV absorption spectra measured before and after CO_2 laser pumping. In the region 230–300 nm, the peak of the UV absorption spectrum for a 300 K thermal sample of HFB is at 230 nm. Following IRMPA the UV absorption is shifted to longer wavelength and is zero at 230 nm.[33,34] These measurements have been made at pressures of 30 Torr[33] and 2 Torr[34] of HFB. In the latter case the laser fluence was 0.18 J cm^{-2}; in the other it was not reported. Our measurements have been made at lower total pressures (<1 Torr) and a higher fluence of ~0.8 J cm^{-2}. We expect that under our experimental conditions all HFB molecules will absorb.

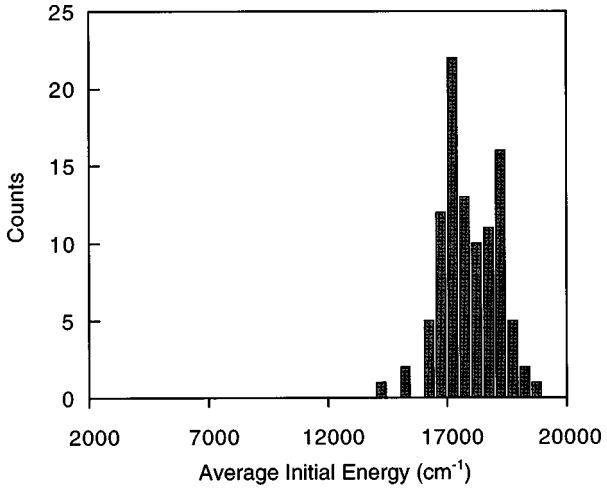

FIG. 2. Histogram of average energy absorbed per molecule recorded for 100 pulses of the CO_2 laser.

We have proceeded by analyzing our IRMPA-IRF data on the basis of this assumption. This leads to a particular value of $\overline{n}$, and hence average initial energy, that determines the slope of the $\langle\langle \Delta E \rangle\rangle$ vs E curve. By comparing the $\langle\langle \Delta E \rangle\rangle$ vs E curve obtained from the IRMPA-IRF experiments for Ar with that obtained from the IC-IRF experiments we have a check on the validity of this assumption.

From measurements of the laser fluence before, Φ_{in}, and after, Φ_{out}, the cell (with corrections for attenuation from cell windows), the average absorbed energy, $\langle\langle Q \rangle\rangle$, can be calculated via the relationship[19]

$$\langle\langle Q \rangle\rangle = \frac{\Phi_{in}}{NL} \ln\left(\frac{\Phi_{in}}{\Phi_{out}}\right),$$

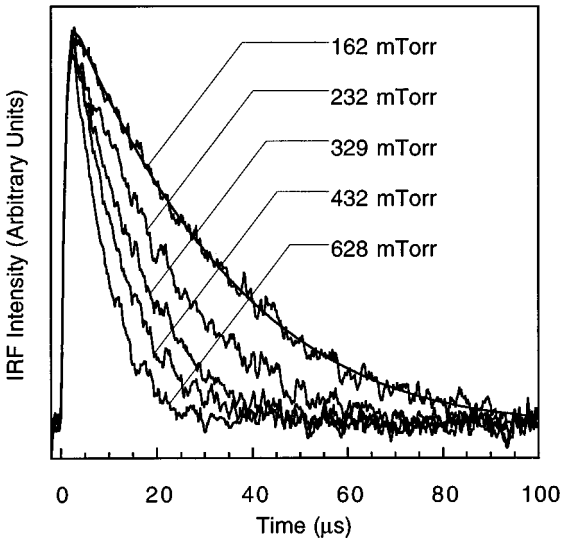

FIG. 3. Infrared fluorescence decay curves for excited HFB prepared by CO_2 laser radiation in the presence of the indicated pressures of argon collider gas. $P_{HFB} = 2.5$ mTorr.

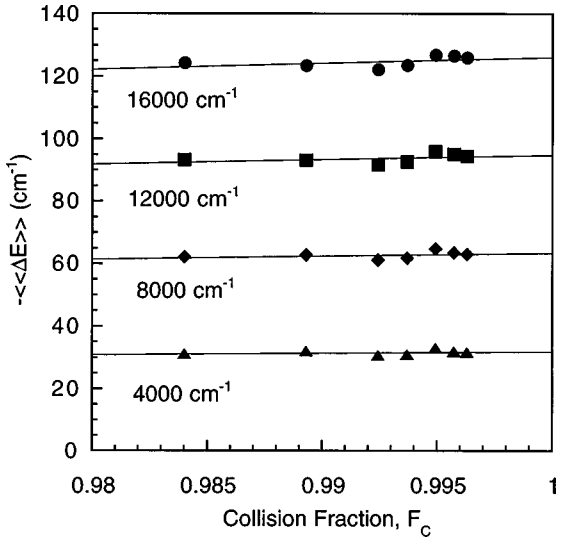

FIG. 4. Average energy transferred per collision as a function of collision fraction for indicated internal energies.

where N is the concentration of the molecule of interest in the cell, and L is the cell length. This equation is valid for a collimated laser beam and an absorption of $<10\%$.[19] When all molecules are excited, as assumed in this study (see above), then $\langle\langle Q\rangle\rangle$ is equal to $\langle\langle E\rangle\rangle$ at time zero. For the laser fluence and pressures used in these experiments the distribution of average initial excitation energies for HFB is shown in Fig. 2. This figure shows the average excitation energy to be $16\,000\pm1500\ \mathrm{cm}^{-1}$.

Decay traces at various bath gas pressures were recorded with a constant HFB pressure of 2.5 mTorr. This very low pressure was necessary to minimize blackbody radiation and to avoid any errors associated with large temperature rises within the cell. Higher pressures also led to shock waves in the cell. The low HFB pressures used increase the accuracy of the data analysis, which involves an extrapolation to zero collision fraction of HFB. IRF traces typical of those observed in the IRMPA experiments are shown in Fig. 3 (a fitted curve is shown on one of the decay traces). Simple random walk simulations show that at the total pressures and timescale of the experiments, wall collisions are insignificant. Plots of $\langle\langle\Delta E\rangle\rangle$ versus collision fraction, F_c, at selected energies are shown in Fig. 4. The parameters for $\langle\langle\Delta E\rangle\rangle$ extracted from the extrapolation of these plots are presented in Table II.

B. UV excitation (IC-IRF) experiments

The UV photophysics of HFB has been investigated by many authors.[35] After excitation with an excimer laser at both 193 nm (ArF) and 248 nm (KrF) hexafluorobenzene undergoes rapid internal conversion to the electronic ground state with almost unit quantum efficiency to produce an ensemble of highly vibrationally excited molecules. This method of initial state preparation has been used previously to excite HFB for collisional energy transfer studies.[13,36–38]

Decay traces at various Ar pressures were recorded with a constant HFB pressure of 50 mTorr. These traces are analyzed to obtain $\langle\langle\Delta E\rangle\rangle$ as discussed above. The parameters k_1 and k_2 for the $\langle\langle\Delta E\rangle\rangle$ function obtained are shown in Table II.

TABLE II. Energy dependence of the average energy transferred per collision for highly excited HFB deactivated by argon.

Excitation method	k_1	k_2	$-\langle\langle\Delta E\rangle\rangle$ at 15 000 cm^{-1} (cm^{-1})
UV-IC	8.11 (8.16)[a]$\times10^{-3}$	1.13×10^{-6}	126 ± 9
IRMPA	8.13 (8.20)[a]$\times10^{-3}$	4.29×10^{-7}	122 ± 5

[a]Values in parentheses are from fits to the linear form, $-\langle\langle\Delta E\rangle\rangle = k_1\langle\langle E\rangle\rangle$.

V. DISCUSSION

The energy transfer parameters, determined from our UV-IC preparation of highly excited HFB, can be directly compared with previous studies using the same preparation technique[13,37] and also theoretical calculations.[14] A summary of $\langle\langle\Delta E\rangle\rangle$ values obtained from the studies above, along with the our values, is shown in Table III. Figure 5 shows the $\langle\langle\Delta E\rangle\rangle$ vs $\langle\langle E\rangle\rangle$ curves for the present work along with other experimental and theoretical studies based on the deactivation of highly excited HFB by argon. The error bars on our UV-IC data indicate two standard errors which have been determined from the error in the extrapolation of the $\langle\langle\Delta E\rangle\rangle$ vs F_c curves (see above) and the error determined between different runs. The $\langle\langle\Delta E\rangle\rangle$ vs $\langle\langle E\rangle\rangle$ curve for Damm *et al.*[13] was estimated from their Fig. 9, while the data points for the theoretical curve were estimated from Fig. 4 of Lenzer *et al.*[14] The theoretical points of Lenzer *et al.*[14] have been joined by a line for illustrative purposes. Although the work of Ichimura *et al.*[37] was assessed by Damm *et al.*[13] to be obsolete due to an incorrect calibration curve, it has been included for completeness.

As evidenced by Fig. 5, our $\langle\langle\Delta E\rangle\rangle$ vs $\langle\langle E\rangle\rangle$ curve is lower than that of Damm *et al.*,[13] but larger than that of Ichimura *et al.*[37] The theoretical calculations by Lenzer *et al.*[14] are in close agreement with our data.

Considerable debate exists over the functional form of the $\langle\langle\Delta E\rangle\rangle$ vs $\langle\langle E\rangle\rangle$ curves. The results of Damm *et al.*[13]

TABLE III. Average energy transferred per collision, $-\langle\langle\Delta E\rangle\rangle$ (cm^{-1}) for deactivation of HFB by argon.

		$-\langle\langle\Delta E\rangle\rangle$ (cm^{-1})			
		Average internal energy, $\langle\langle E\rangle\rangle$ (cm^{-1})			
Excitation method	Ref.	51 800[a]	40 300[b]	24 000	15 000
UV-193 nm	37	196	153	91	61
UV-193 nm	13	540	~476[c]	~333[c]	~190[c]
UV-248 nm	this work		327	198	126
IRMPA	this work			194	122
theory-QCT[d]	14			149	

[a]Photon energy at 193 nm.
[b]Photon energy at 248 nm.
[c]Estimated from Fig. 9 of Damm *et al.*[13]
[d]Quasiclassical trajectory calculations.

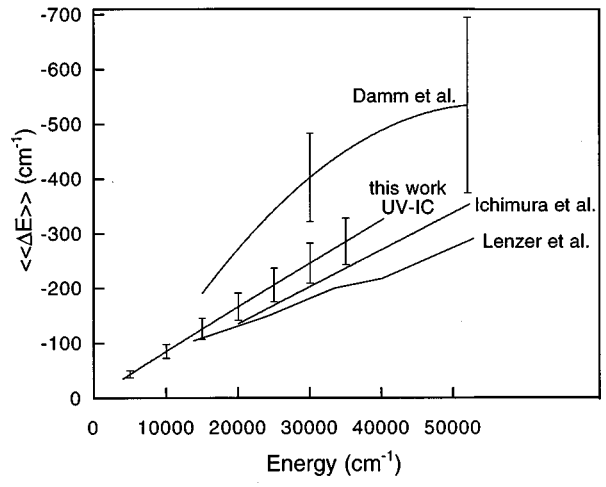

FIG. 5. Summary of $\langle\langle \Delta E \rangle\rangle$ vs $\langle\langle E \rangle\rangle$ curves for the deactivation of highly excited HFB by Ar collider gas.

indicate that there is a definite roll-off with increasing energy. Other authors have even seen these $\langle\langle \Delta E \rangle\rangle$ curves completely roll over ($\langle\langle \Delta E \rangle\rangle$ values decrease with increasing energy).[21] Our assumed functional form for $\langle\langle \Delta E \rangle\rangle$ consists of two parameters, k_1 describing the linear term and k_2 describing any curvature. The UV-IC data obtained in this study show k_2 to be insignificant in comparison with k_1 (see Table II). Although fitting parameters have been used which will model any roll-off that possibly exists, the experimental data suggest $\langle\langle \Delta E \rangle\rangle$ to be essentially linear with energy. The magnitude of the nonlinear term compared with the linear term, obtained in this study, is illustrated through a comparison of the ratios of these two terms. The value of this ratio was found to be $<5\%$ (calculated when the average energy has fallen to half its initial value). Hence, these parameters reveal $\langle\langle \Delta E \rangle\rangle$ to be essentially linear with energy.

$\langle\langle \Delta E \rangle\rangle$ vs $\langle\langle E \rangle\rangle$ curves for both the IRMPA and UV-IC preparative methods are shown in Fig. 6. Errors on the plot represent standard deviations determined from the extrapolation of $\langle\langle \Delta E \rangle\rangle$ vs F_c curves and errors observed between runs. Figure 6 clearly shows that the two experimental results agree well with each other.

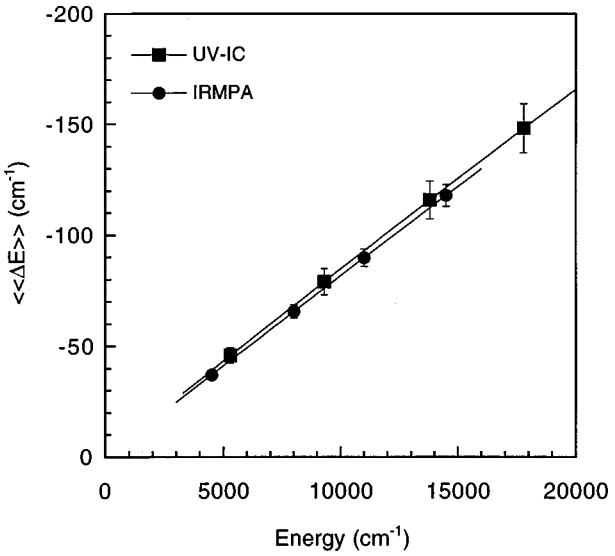

FIG. 6. $\langle\langle \Delta E \rangle\rangle$ vs $\langle\langle E \rangle\rangle$ curves for the two different methods of initial state preparation used in this study.

UV excitation followed by rapid internal conversion results in an initial energy distribution similar to that of a thermal vibrational Boltzmann distribution shifted by the excitation wavelength ($\sim 40\,300\ \mathrm{cm}^{-1}$). On the other hand, IRMPA produces a broader distribution since a HFB molecule can absorb an integer number of photons centered around the average number of photons absorbed per molecule. Although the two methods of initial state preparation produce substantially different initial distributions, the energy transfer parameters obtained by our study are identical within experimental error. This result has previously been postulated from theoretical calculations,[10,11] but until now, no experimental work has substantiated this claim. This is the first direct experimental comparison between the two methods of initial excitation, and demonstrates that IRMPA is a viable method for energy transfer studies.

ACKNOWLEDGMENTS

This work was supported by the Australian Research Council. The authors are grateful for the technical support provided by the staff of the Flinders University Department of Physical Sciences Electronic Workshop and the Adelaide University Department of Chemical Engineering Mechanical Workshop. J.R.G. is grateful for the award of a Ferry Scholarship.

[1] I. Oref and D. C. Tardy, Chem. Rev. **90**, 1407 (1990).
[2] J. R. Barker and M. L. Yerram, in *Multiphoton Processes*, edited by S. J. Smith and P. L. Knight (Cambridge University Press, Cambridge, 1988), p. 201.
[3] T. C. Brown, K. D. King, J.-M. Zellweger, and J. R. Barker, Ber. Bunsenges. Phys. Chem. **89**, 301 (1985).
[4] J.-M. Zellweger, T. C. Brown, and J. R. Barker, J. Chem. Phys. **83**, 6251 (1985).
[5] J.-M. Zellweger, T. C. Brown, and J. R. Barker, J. Chem. Phys. **83**, 6261 (1985).
[6] J.-M. Zellweger, T. C. Brown, and J. R. Barker, J. Phys. Chem. **90**, 461 (1986).
[7] B. Abel, H. Hippler, and J. Troe, J. Chem. Phys. **96**, 8863 (1992).
[8] B. Abel, H. Hippler, and J. Troe, J. Chem. Phys. **96**, 8872 (1992).
[9] E. A. Coronado and J. C. Ferrero, J. Phys. Chem. A **101**, 9603 (1997).
[10] E. A. Coronado, C. A. Rinaldi, G. F. Velardez, and J. C. Ferrero, Chem. Phys. Lett. **227**, 164 (1994).
[11] E. A. Coronado and J. C. Ferrero, Chem. Phys. Lett. **257**, 674 (1996).
[12] C. A. Rinaldi, J. C. Ferrero, M. A. Vázquez, M. L. Azcárate, and E. J. Quel, J. Phys. Chem. **100**, 9745 (1996).
[13] M. Damm, H. Hippler, H. A. Olschewski, J. Troe, and J. Willner, Z. Phys. Chem., Neue Folge **166**, 129 (1990).
[14] T. Lenzer, K. Luther, J. Troe, R. G. Gilbert, and K. F. Lim, J. Chem. Phys. **103**, 626 (1995).
[15] T. Lenzer and K. Luther, Ber. Bunsenges. Phys. Chem. **101**, 581 (1997).
[16] K. L. Poel, Z. T. Alwahabi, and K. D. King, Chem. Phys. **201**, 263 (1995).
[17] K. L. Poel, Z. T. Alwahabi, and K. D. King, J. Chem. Phys. **105**, 1420 (1996).
[18] K. L. Poel, C. M. Glavan, Z. T. Alwahabi, and K. D. King, J. Phys. Chem. A **101**, 5614 (1997).
[19] V. N. Bagratashvili, V. S. Letokhov, A. A. Makarov, and E. A. Ryabov, *Multiple Photon Infrared Laser Photophysics and Photochemistry* (Harwood, London, 1985).
[20] L. A. Miller and J. R. Barker, J. Chem. Phys. **105**, 1383 (1996).
[21] B. M. Toselli, J. D. Brenner, M. L. Yerram, W. E. Chin, K. D. King, and J. R. Barker, J. Chem. Phys. **95**, 176 (1991).

[22] J. F. Durana and J. D. McDonald, J. Chem. Phys. **64**, 2518 (1977).
[23] J. R. Barker and B. M. Toselli, Int. Rev. Phys. Chem. **12**, 305 (1993).
[24] T. Beyer and D. F. Swinehart, Commun. ACM **16**, 379 (1973).
[25] V. J. Eaton and D. Steele, J. Mol. Spectrosc. **48**, 446 (1973).
[26] R. A. R. Pearce, D. Steele, and K. Radklife, J. Mol. Struct. **15**, 409 (1973).
[27] P. W. Atkins, *Physical Chemistry* (Oxford University Press, Oxford, 1994).
[28] P. R. Bevington, *Data Reduction and Error Analysis for the Physical Sciences* (McGraw–Hill, New York, 1969).
[29] W. H. Press, S. A. Teukolsky, W. T. Vetterling, and B. P. Flannery, *Numerical Recipes in FORTRAN* (Cambridge University Press, Cambridge, 1992).
[30] P. D. Neufeld, A. R. Janzen, and R. A. Aziz, J. Chem. Phys. **57**, 1100 (1972).
[31] V. N. Bagratashvili, Y. G. Vainer, V. S. Doljikov, V. S. Letokhov, A. A. Makarov, L. P. Malyavkin, E. A. Ryabov, and E. G. Silkis, Opt. Lett. **6**, 148 (1981).
[32] V. N. Bagratashvili, Y. G. Vainer, V. S. Doljikov, S. F. Koliakov, A. A. Makarov, L. P. Malyavkin, E. A. Ryabov, E. G. Silkis, and V. D. Titov, Appl. Phys. **22**, 101 (1980).
[33] S. Speiser and E. Grunwald, Chem. Phys. Lett. **73**, 438 (1980).
[34] X. Chen, L. Li, F. Sun, and C. Zhang, Acta Opt. Sin. **4**, 781 (1984).
[35] D. Phillips, J. Chem. Phys. **46**, (1967).
[36] T. Ichimura, Y. Mori, N. Nakashima, and K. Yoshihara, J. Chem. Phys. **83**, 117 (1985).
[37] T. Ichimura, M. Takahashi, and Y. Mori, Chem. Phys. Lett. **114**, 111 (1987).
[38] C. A. Michaels, Z. Lin, A. S. Mullin, H. C. Tapalian, and G. W. Flynn, J. Chem. Phys. **106**, 7055 (1997).